Heterodyne and Coherent Optical Fiber Communications: Recent Progress

TAKANORI OKOSHI, MEMBER, IEEE

Invited Paper

Abstract—**The technical significance, history of research and development, relevant technical tasks, and recent progress in heterodyne and coherent optical fiber communications are described. The achievements of 1-MHz frequency stability (peak-to-peak) and 0.1-MHz spectral purity (3-dB spectral width) with semiconductor lasers have been two principal motivations that accelerated the research and development. Rapid progress in the single-polarization single-mode fiber technology is also encouraging. The bit-error rate of a PCM–ASK/heterodyne optical communication system has been measured as a function of the received signal level, showing a good error performance close to the quantum-noise limitation.**

I. Introduction

A. General Background—Why Heterodyne Now?

THE PRESENT optical fiber communications are in a sense as primitive as the radio communications prior to 1930. The reason is that neither of these make use of the phase information of the carrier; in other words, both of these are noncoherent communications.

The modulation/demodulation scheme being employed in the present standard optical fiber communications is often called the intensity-modulation/direct-detection (hereafter IM/DD) scheme. The term IM stems from two facts: 1) that the light intensity (not the amplitude) is modulated linearly with respect to the input signal voltage; and 2) that basically no attention is paid to the phase of the carrier. (The original spectral spread of the optical carrier is usually much wider than the spread due to modulation.) The term DD stems from that the signal is detected directly at the optical stage of the receiver; neither the frequency conversion (heterodyne scheme) nor sophisticated signal processing at lower frequencies are performed.

On the other hand, in the history of radio communications, the heterodyne scheme became common since 1930, and is now widely used even in pocket radio sets. Sophisticated coherent modulations such as FM, PM, frequency-shift keying (FSK), and phase-shift keying (PSK) are also widely used in broadcasting and communications.

Here a question arises: will the IM/DD system continue to be predominating in optical communications for at least ten years from now? Or will it gradually retire to yield its present position to more sophisticated heterodyne and/or coherent systems?

The IM/DD system has a great advantage in system simplicity and low cost. On the other hand, some applications of the optical fiber communications exist in which a long repeater separation is our primary concern; an example is the optical fiber communications between islands. In such a case, the improvement of the equivalent receiver sensitivity by a heterodyne-type receiving technique, or by coherent modulation/demodulation scheme such as PCM–FSK or PCM–PSK may become advantageous, even at the sacrifice of simplicity and low cost. Especially noteworthy is that (as seen later) the sensitivity improvement is particularly dramatic ($10 \sim 25$ dB) at the $1.5 \sim 1.6$-μm wavelength region [1], [2], where the silica-fiber loss becomes minimum (~ 0.2 dB/km) whereas good photodetectors (for the DD scheme) are not available. The sensitivity improvement of 20 dB will result in a repeater-separation elongation of 100 km when the fiber loss is 0.2 dB/km.

The above expectation on the receiver-sensitivity improvement is the principal motivation underlying the present effort toward the heterodyne/coherent optical fiber communications. On the other hand, it is accepted by all the specialists that the IM/DD systems will never retire, because the heterodyne/coherent systems are, and will continue to be, rather expensive.

B. Historical Background

In reviewing the history of this topic, we must first distinguish optical communications and optical fiber communications. The heterodyne-type optical communication is not a new topic. The optical communication systems conceived by Bell Laboratories investigators in the late 1960's were heterodyne systems [3] imitating millimeter-wave communications. However, those systems were assumed to use lens waveguides and gas lasers, and look far from practical at present. After the advent of practical fibers and semiconductor lasers in 1970, the IM/DD optical fiber communications became predominant; the heterodyne scheme had been given up until 1978 mainly because of the poor spectral purity of semiconductor lasers.

The second phase of the research started in Japan in

Manuscript received March 24, 1982.

The author is with the Department of Electronic Engineering, University of Tokyo, 7-3-1 Hongo, Bunkyo-ku, Tokyo 113 Japan.

0018-9480/82/0800-1138$00.75

1978 [4]. At present, the research toward the heterodyne/coherent systems is performed in more than ten laboratories in the world.

C. Purpose of this Paper

The purpose of this paper is to describe the technical advantages and relevant technical tasks of heterodyne and/or coherent optical fiber communications, and to review the recent progress in the research and development toward those.

A comment is added here on the relation of "heterodyne" and "coherent" schemes. The heterodyne detection is *practically*[1] a premise for the coherent communications. However, the coherent modulation is never a premise for the heterodyne system; an IM signal could also be detected by a heterodyne scheme. Because PCM signals are mainly considered in this paper, such a case will be referred to as the PCM amplitude-shift keying (ASK) or PCM on–off keying (OOK) heterodyne envelope-detection scheme.

II. Technical Advantages of Heterodyne and/or Coherent System

A. Improvement of Equivalent Receiver Sensitivity

The greatest advantage of a heterodyne/coherent system is the improvement of the equivalent receiver sensitivity, more exactly, the reduction of the minimum receiving signal level for achieving a prescribed bit-error rate, for example 10^{-9}.

This improvement is attributed to two effects [5]. One is the improvement of the S/N (signal-to-noise ratio) at the output end of the receiver preamplifier by the use of the heterodyne scheme. The other is the improvement brought about by the use of a coherent modulation/demodulation scheme [6].

B. Sensitivity Improvement by Various Detection Schemes Including Heterodyning

Various detection schemes for achieving high S/N are first compared [7]. In an optical detection, i.e., in an opto-electronic (OE) signal conversion, an absolute S/N limitation exists due to the fact that light is not continuous but consists of photons, which produce a flow of discrete electrons at the electrical terminals of the photodetector. Therefore, an ideal photodetection is not a noise-free detection but a quantum-noise-limited detection, giving, as shown in the Appendix,

$$(S/N)_{\text{ideal}} = P_s/2hf\Delta f \tag{1}$$

where P_s denotes the received signal power, h is Planck's constant ($=1.38\times10^{-34}$ J·s), f the optical signal frequency, and Δf the bandwidth of the receiver.

[1]A nonheterodyne coherent communication is imaginable. For example, an all-optical PCM–PSK detector could be constructed by using an interferometer-type differential PSK detector, and also an all-optical PCM–FSK detector by using two optical resonators. However, system analyses tell that practically such nonheterodyne detection schemes can not offer the good receiver sensitivity featuring these coherent modulation/demodulation schemes.

Four methods (including the heterodyne method) are available to realize a nearly quantum-noise-limited detection.

1) Direct Detection Using a Low-Noise Avalanche Photo-Diode (APD): In this case

$$\frac{S}{N} = \frac{CM^2}{AM^{2+x}\Delta f + B\Delta f} \tag{2}$$

where

$$A = 2e(\eta e/hf)P_s \tag{3}$$

$$B = 4kTF/R_L \tag{4}$$

$$C = [(\eta e/hf)P_s]^2 \tag{5}$$

M denotes the avalanche multiplication factor of the APD, x the excess noise factor, η the quantum efficiency of the detector, k the Boltzmann constant, T the receiver temperature, F the noise figure of the preamplifier, and R_L the load resistance to the APD. If $M\to\infty$ and $x\to 0$, (2) agrees with (1).

The value of M could be as large as 100. However, $x=0.2\sim0.4$ for Si APD, $x=0.8\sim1$ for Ge APD, and $x=0.5\sim0.7$ for GaInAsP APD. Therefore, an S/N close to (1) can be obtained only at wavelengths below 1 μm where Si-APD can be used. The S/N is much deteriorated at 1.3 μm or 1.55 μm where Ge APD or III–V compound APD must be used.

2) The Use of Low-Noise Laser Amplifier: We consider a system consisting of a laser preamplifier and an OE converter. In this case

$$\frac{S}{N} = \frac{GC^2}{AG^2\Delta f + B\Delta f + N_a} \tag{6}$$

where G denotes the power gain and N_a the excess noise such as the spontaneous emission noise. If $G\to\infty$ and $N_a\to 0$, the S/N becomes equal to (1). In experiments using GaAlAs lasers, an S/N fairly worse than (1) is observed (see the final paragraph of Section VII).

This method is significant especially when the optical bandwidth can effectively be limited to the signal bandwidth. This is not the case when the laser amplifier is followed by an APD and a baseband amplifier; in this case the spontaneous noise of the laser in a very wide frequency band will generate a large excess noise in the detector due to mixing effect. Practically, therefore, the laser amplifier had better be followed by a heterodyne receiver which offers a sharp optical frequency selectivity.

3) Use of a Photon-Counting Technique: In a photon-counting system, the excess receiver noise can be separated from the intrinsic quantum noise by pulse-height analysis, because these two kinds of noise appear at different height levels as shown in Fig. 1. However, the photon-counting techniques available at present do not offer a response quick enough for practical communications purpose.

4) Heterodyne Detection Using a Photo-Diode (PD): In this case, an APD and a PD make no difference in S/N when the local oscillator power P_{LO} is sufficient. The S/N

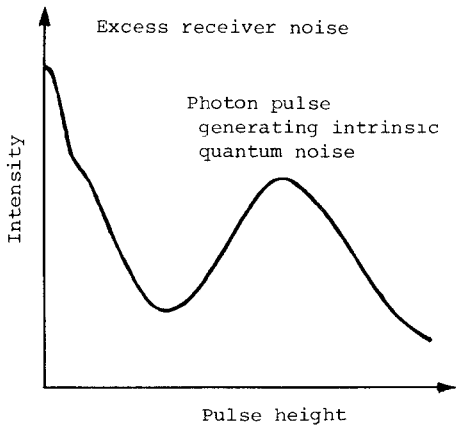

Fig. 1. Principle of the photon-counting technique for achieving quantum-noise-limited detection.

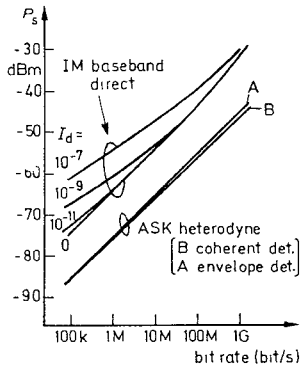

Fig. 2. Comparison of the minimum receiving signal level for the IM/DD and ASK/heterodyne schemes in the long-wavelength region (BER $=10^{-9}$, $x=1.0$). The values of I_d, photodetector-dark current, are given in amperes.

is given as

$$\frac{S}{N}=\frac{C'}{A'\Delta f+B\Delta f} \tag{7}$$

where

$$A'=2e(\eta e/hf)P_{\mathrm{LO}} \tag{8}$$

$$C'=(\eta e/hf)^2 P_{\mathrm{LO}}P_s \tag{9}$$

and it is assumed that $P_s \ll P_{\mathrm{LO}}$. When $P_{\mathrm{LO}}\to\infty$, the S/N becomes again equal to (1). Practically, enough local power P_{LO} can be obtained and injected by using a semiconductor laser.

C. Sensitivity Improvement by Heterodyne Scheme

It is thus found that at least at present, the heterodyne scheme is the only practical method with which a nearly quantum-noise limited detection can be realized. As shown in Section VII, an S/N about 1 dB lower than the quantum-noise limit can actually be obtained.

Fig. 2 shows an example from the results of analyses comparing the IM/DD and ASK/heterodyne systems [5]. The ordinate shows the receiving signal level necessary to obtain a BER (bit-error rate) of 10^{-9}. The abscissa is the information-transmission rate (bit rate) of the PCM signal.

The lower two curves show the required signal levels for

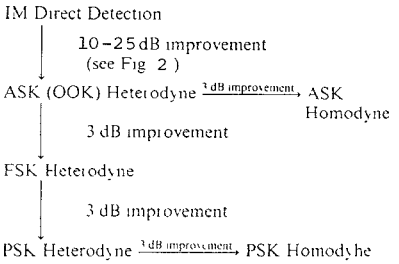

Fig. 3. Improvement of the minimum receiving signal level by various coherent modulation/demodulation schemes.

ASK/heterodyne cases: curve A for the envelope (noncoherent) detection and B for the coherent detection. It is found that in an ASK system the advantage in the use of the coherence is rather small.

The upper four curves show the required signal level for the IM/DD case. The excess noise factor x is assumed to be 1.0, corresponding to long-wavelength (1.3 ~ 1.6 μm) detectors. The parameter I_d denotes the dark current (in amperes), which is not considered in (2) for simplicity. In the present technology, $I_d \simeq 10^{-10}$ A for Si APD, but $I_d \simeq 10^{-6}$ A for Ge APD and $I_d \simeq 10^{-8}$ A for III–V compound APD.

We find in Fig. 2 that the improvement in the required signal level, from the IM/DD scheme to the ASK/heterodyne scheme, ranges between 10 and 25 dB. Generally speaking, the advantage of the heterodyne detection is emphasized at long wavelengths (1.3 ~ 1.6 μm) where x and I_d are large, and at low signal bit-rate. This means that it is especially advantageous when a very long repeater separation is required.

D. Sensitivity Improvement by Coherent Modulation Schemes

The technical significance of the heterodyne scheme lies partly in that it is a premise for the optical communications using a coherent modulation such as PCM–FSK. The sensitivity improvement by these schemes had been known in general communication theory [8]; it was modified and applied to optical communication systems first in [6], and later in [5] taking into the receiver design [9] into account.

Fig. 3 summarizes the improvement of the minimum receiving signal level for obtaining a prescribed BER by various heterodyne and coherent communication schemes [2]. By the use of ASK/heterodyne scheme, an improvement of 10 ~ 25 dB can be expected as compared with the IM/DD scheme (see Fig. 2). As compared with ASK/heterodyne, 3-dB further improvement can be expected with FSK/heterodyne scheme, and 3-dB further improvement can be expected with a PSK/heterodyne scheme [5].

Still further 3-dB improvement could be obtained if we realize ASK/homodyne or PSK/homodyne systems, as compared with the corresponding heterodyne systems. However, for the time being these seem technically rather difficult, because a stable local oscillator output synchronized to the received carrier must be reproduced in the receiver, probably by using a deliberate phase-locked loop (PPL) technique, to realize a homodyne system.

On the other hand, 3-dB and 5-dB improvement could be expected if we realize 4-level and 8-level FSK systems, respectively [5] (not shown in Fig. 3). This is possible because, in such cases, we can reduce the signal bit-rate by 1/2 and 1/3, respectively, while still transmitting the same amount of information (see Fig. 2).

E. Frequency-Selectivity Improvement by Heterodyning

The second advantage of a heterodyne system is that the frequency selectivity can much be improved because of the good frequency selectivity of the intermediate frequency (IF) amplifier, which is much sharper than that of an optical filter. Thus, an FDM (Frequency-Division Multiplexing) with very fine carrier separation becomes possible, which allows, for example, an efficient use of the minimum dispersion wavelength region (1.3-μm region) of silica-glass optical fibers. However, in the present state of the art, this advantage can not be emphasized because a part of optical power is lost in the optical multiplexer at the transmitting end when the frequency separation between carriers is small.

An indirect, but practically more important effect of the frequency-selectivity improvement is that the light amplification using a laser preamplifier becomes really advantageous when the effective optical frequency bandwidth is narrowed because the optical background noise outside the signal bandwidth can effectively be suppressed.

III. Relevant Technical Tasks

The following technical difficulties must be overcome before a practical heterodyne and/or coherent systems are realized in future [1], [2], [10], [11].

1) The most important problem is how to stabilize the frequency of semiconductor lasers, which are at present most possibly used as the transmitter as well as the local oscillator (LO). Since a typical IF frequency would be $0.2 \sim 2$ GHz, which is about $10^{-6} \sim 10^{-5}$ times the signal frequency (typically 200 THz), the requirement for the frequency stability is very severe.
2) The spectral purity of the semiconductor laser must also be improved. If the carrier or the LO output is noisy, the frequency or phase fluctuations will deteriorate the bit-error rate, thus raising the required signal level.
3) Practical, simple, and stable ASK, FSK, and PSK modulation/demodulation techniques must be developed.
4) The random fluctuation of the mixer efficiency due to the fluctuation of the polarization state of the received optical signal must be prevented by the use of a polarization maintaining fiber, or by some other appropriate means such as a polarization controlling device at the input end of the receiver and/or a polarization diversity scheme.
5) Although its technical merit has not yet fully been proved, a laser preamplifier should be investigated because it might improve the overall performance of heterodyne receivers in the future.
6) Finally, combining some of or all of the above techniques, experimental systems must be constructed to demonstrate the aforementioned advantages in a practical scale.

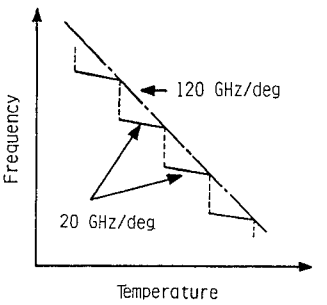

Fig. 4. Typical frequency versus temperature characteristics of a single-mode GaAlAs laser.

In the following four sections, recent progress in the above technical fields will briefly be reviewed except for items (3) and (5). These subjects (modulators and laser amplifiers) seem to belong to the quantum-electronics field, and have been discussed in a detailed and comprehensive manner in a recent review paper which appeared in another IEEE publication [10].

IV. Frequency Stabilization of Semiconductor Lasers

Basically, two methods are available for stabilizing the oscillation frequency of a semiconductor laser. One is the automatic frequency control (AFC) in which the laser temperature is controlled [12], [13], and the other is the AFC controlling the injection current [14], [15]. The temperature-controlled AFC can offer a tunable frequency range of about 30 GHz, which is much wider than that of the current-controlled AFC scheme (~ 0.3 GHz). On the other hand, the latter has a shorter response time (~ 1 μs) than the former (~ 1 s).

As the optical frequency standard for the AFC scheme, a Fabry–Perot etalon is commonly used. However, the use of a molecular standard is also considered and experimented with [16]–[19].

A. Temperature-Controlled AFC Using Fabry–Perot Etalon

Fig. 4 shows a typical temperature dependence of the oscillation frequency of a single-mode, Fabry–Perot type GaAlAs laser. The dashed–dotted line having a slope of 120 GHz/K shows the frequency variation due to the variation of the maximum-gain frequency. However, as far as the laser oscillates in a given mode, the frequency cannot vary so steeply, except along the solid lines having a slope of 20 GHz/K, which corresponds to the temperature dependence of the refractive index and the thermal expansion of the laser cavity. To follow the overall variation of 120 GHz/K, the oscillation frequency jumps between modes. Still, we can tune the stabilized frequency over about 30 GHz within a single mode between two jumping frequencies. This frequency range is expected to be widened further when distributed feedback (DFB) lasers become practically available in near future.

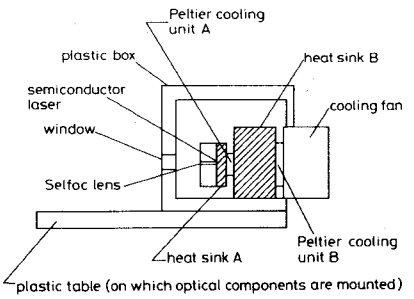

Fig. 5. Construction of temperature-controlled laser unit.

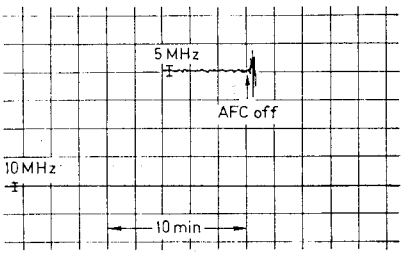

Fig. 6. Drift of the semiconductor-laser frequency in the AFC state (upper inset: enlarged ordinate scale) obtained with a temperature-controlled scheme.

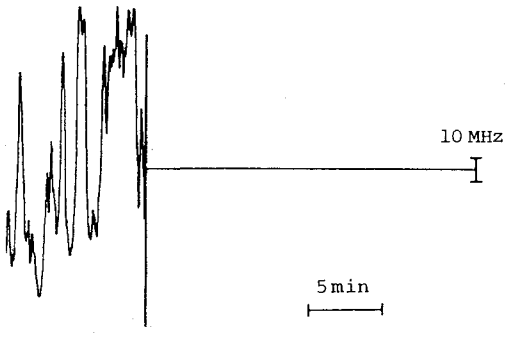

Fig. 7. Drift of the semiconductor-laser frequency in freerunning and AFC states obtained with a current controlled scheme (after Favre and LeGuen [15]).

Frequency stability of 1 MHz has been achieved by using a double-loop AFC system [13]. In this system, the laser temperature is controlled by a Peltier effect cooling element to give a prescribed oscillation frequency. The feedback circuit consists of a Fabry–Perot etalon, two photodiodes, a differential amplifier, and Peltier cooling element. The light from the laser is divided into two parts. One part is directly detected by one photodiode, whereas the other part is led to the Fabry–Perot interferometer and its throughput is detected by the other photodiode. The outputs of the two photodiodes are input to a differential amplifier, whose output signal controls the Peltier cooling element.

On the other hand, to assure a high stability of the AFC system, another feedback loop stabilizes the temperature of the heat sink of the first Peltier element, so that it is constant regardless of external disturbances. The construction of the AFC laser unit is shown in Fig. 5.

Fig. 6 shows the frequency drift of the stabilized laser in the AFC state. An expanded graph is shown in the upper part of this figure. We find that the frequency is stabilized within 1 MHz. The 1-MHz stability could be maintained for more than 2 h. The frequency tunability within the passband of the etalon (1 GHz) was also attained, without decreasing the frequency stability [13].

B. Current-Controlled AFC Using Fabry–Perot Etalon

The frequency stability of 1 MHz has also been obtained by a current-controlled AFC scheme [15]. Fig. 7 shows the frequency fluctuation in a free-running state (left half) and with AFC (right half). The current-controlled AFC is superior in its high cutoff response frequency, and hence the possibility of attaining higher loop gain. The drawback is the narrow tunable frequency range and the danger of damaging the laser due to runaway. The latter problem is particularly serious because presently available lasers are weak in abrupt current fluctuation and current overload.

C. AFC Schemes Using Molecular Standard

In Figs. 6 and 7, the ordinates show the output voltage of the detector for the Fabry–Perot interferometer throughout, but it is scaled with the frequency deviation on the assumption that the Fabry–Perot etalon is stable enough during the period of measurement.

The resonant frequency of a Fabry–Perot etalon is given as

$$f = mc/2nL \tag{10}$$

where m denotes an integer, c the light velocity, n the refractive index, and L the length of the etalon. If we use fused quartz ($n \doteqdot 1.5$) in the etalon, the temperature coefficient of n predominates over that of L by about one order of magnitude, and $|dn/dT| \simeq 10^{-5}$/K. Therefore, at $f =$ 300 THz, $|df/dT| \simeq 2$ GHz/K. This means if $\Delta T < 0.01$ K is attained, the real frequency fluctuation can be reduced to 20 MHz.

The stability of 20 MHz is probably satisfactory for a transmitting laser. (For the LO laser, we can use an AFC using an IF discriminator, and the difficulty is much less.) If otherwise, we have to relay upon a molecular frequency standard.

Several experiments of semiconductor-laser stabilization by moleculer standard have so far been reported.

1) Stabilization of GaAlAs laser with respect to H_2O vapor absorption line [16]. The obtained stability is 5 MHz.
2) Stabilization of GaAlAs laser using Lamb dip in Cs vapor [17] [18]. The obtained stability is 100 kHz for 1 min.
3) Stabilization of GaAlAs laser by a Fabry–Perot etalon controlled by a Lamb-dip-stabilized He–Ne laser [19]. The obtained stability is 7 kHz $< \sigma <$ 700 kHz for 10 ms $< \tau <$ 8.5 min, where σ denotes the square root of the Allan variance and τ the integration time.

The above data tell that much improvement in the performance will be required before the use of a molecular standard becomes definitely advantageous.

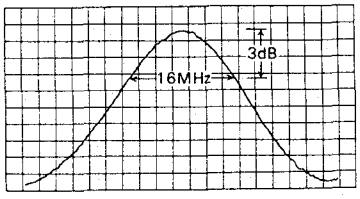

Fig. 8. A measured frequency spectrum of a GaAlAs laser (reflection-free state).

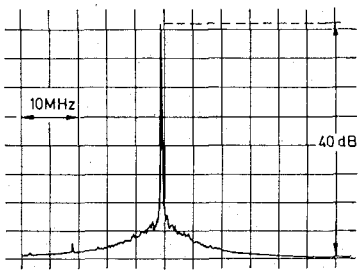

Fig. 9. A measured frequency spectrum of a GaAlAs laser with reflection of an appropriate magnitude and from an appropriate distance.

V. Measurement and Improvement of Spectral Purity of Semiconductor Lasers

A. High-Resolution Spectral Analysis

Late in the 1970's, some investigators noticed that the spectral spread, that is, the 3-dB bandwidth of the best-stabilized semiconductor lasers was sometimes as narrow as several megahertz. This finding, together with the achievement of good frequency stability as described in [12], was the very motivation that forced engineers to start the research of heterodyne-type optical fiber communications.

However, conventional spectroscopy techniques cannot offer a spectral resolution fine enough for determining the shape of such a sharp spectrum. A new fine-resolution technique called the "delayed self-heterodyne method" has been devised [20] and used in the measurement in many laboratories.

The principle of this method follows. Generally, a high spectral resolution can be offered by a heterodyne-type measuring system. However, the difficulty is that we can not always obtain a stable local oscillator at an arbitrary optical frequency. In this method, therefore, a part of the laser output itself is used as the local oscillator power.

Laser output is divided into two paths. One part is delayed by time τ_d through a single-mode fiber, and is regarded as the local oscillator power. The other part is frequency-shifted by a frequency f_s, which should be much higher than the expected spectral spread to be measured. The throughputs of the two paths are mixed by an avalanche photodiode, and the noise spectrum of the mixer-output is measured by a radio-frequency spectrum analyzer. In this method the frequency resolution-limit is given approximately as τ_d^{-1}, which can easily be made below 100 kHz [15], [20].

The typical 3-dB spectral spread of a GaAlAs single-mode laser obtained by using the above system is about 10 MHz, as far as the effect of optical reflection is carefully removed by using an optical isolator [20]. Fig. 8 shows an example of such a spectrum.

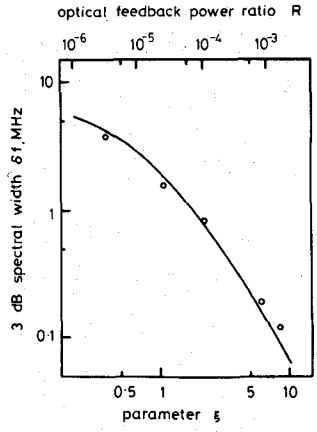

Fig. 10. The 3-dB spectral width as a function of feedback power ratio R, or a parameter ξ which is proportional to $\tau R^{1/2}$.

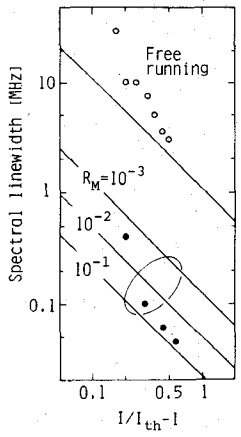

Fig. 11. The 3-dB spectral width obtained with a grating type reflection scheme (after Saito and Yamamoto [21]).

B. Spectrum Narrowing by Optical Feedback

On the other hand, it has been found experimentally that a certain amount of optical feedback (typically −40 dB) from an appropriate distance (typically 50 cm) often narrows the spectral spread of a semiconductor laser appreciably, in some cases below 100 kHz [1], [2], [15], [21]. In other words, the spectral purity can be improved by addition of an external long-cavity resonator. Fig. 9 shows an example of such a sharpened spectrum [2].

Recently, a theory was presented from which a simple formula giving the spectrum-narrowing ratio can be derived [22]. The measured and theoretical values of 3-dB spectral width are compared in Fig. 10, where the upper and lower abscissas show the feedback power ratio R and a parameter ξ which is proportional to $\tau R^{1/2}$, respectively, where τ denotes the round-trip time of the feedback light. The delayed self-heterodyne method [20] has been used in the experiment. The measured values of the 3-dB spectral width (small circles) are in good agreement with the theoretical curve.

Fig. 11 shows the result of another experiment using a diffraction grating in the feedback loop [21]. In the ab-

scissa, I and I_{th} denote the bias and threshold current, respectively. The slant lines show theoretical linewidth, where the parameter R_M denotes the reflection coefficient of the diffraction grating. Measured values are shown by small circles and dots.

VI. Polarization Matching Between Signal and Local-Oscillator Beams

The next problem is how to achieve the polarization matching between the received signal and the local oscillator beams. In an ordinary axially symmetrical optical fiber, the polarization state of the propagated wave is subject to unstable fluctuations when ambient conditions change only very slightly. In a heterodyne system, this fluctuation is serious because the mixer efficiency is critically dependent upon the polarization matching between the signal and the local oscillator beams. Various methods have been devised to overcome this difficulty.

A. Polarization Correction and Polarization Diversity

The first method is the active correction of the polarization state at the input end of the receiver. This has been proposed and experimented with first by Ulrich using electromagnetic fiber squeezers as the polarization-control device [23], and also by Kubota *et al.* who used electrooptic polarization controllers [24]. Another type of the polarization controller consisting of circularly wound and twisted fiber sections has been proposed by LeFevre [25].

The second one is the polarization diversity receiver [1] in which the signals in two polarization states are received independently and added later. However, this has not been experimented with.

B. Single-Polarization and Birefringent Fiber Schemes (General Description)

In the third approach, the polarization is stabilized over the entire length of the fiber waveguide. Such optical fibers are called generically polarization maintaining fibers, or sometimes single-polarization single-mode (SPSM) fibers [26]. The polarization-maintaining schemes can further be classified into three groups.

One approach, which looks at first the final (and even easy) solution, is to devise an axially nonsymmetrical structure in which one of the two orthogonal HE_{11} modes is cut off; this might be called the "absolutely SPSM" scheme. The "side-pit fiber" described in Section VI-F was proposed [27] and fabricated [28] first for this purpose. However, to make a practical, really SPSM fiber by the side index-pit scheme is rather difficult except when the core-cladding refractive-index difference is very large, above several percent [27]. To achieve the really SPSM characteristics more easily, the "side-tunnel" fiber has been proposed [29] and being fabricated (see Section VI-F).

The second scheme has a longer history and is most practical at present. It is to make the difference of the propagation constants of orthogonally polarized two HE_{11} modes (hereafter called HE_x and HE_y modes, where the suffixes denote the direction of the electric field) as large as possible. This can be achieved by an axially nonsymmetrical refractive-index distribution [30]–[33], or by a nonsymmetrical stress distribution [34]–[39]. Such fibers are called linearly "birefringent" fibers, or also SPSM fibers because a launched HE_{11} mode can be propagated in the given polarization over a long distance when the propagation-constant difference is large.

The difference between the propagation constants of the HE_x and HE_y modes, $\delta\beta = \beta_x - \beta_y$, is called the polarization birefringence or modal birefringence. A normalized quantity called the normalized birefringence

$$B = \delta\beta/\beta_{av} = 2(\beta_x - \beta_y)/(\beta_x + \beta_y) \tag{11}$$

and the beat length between the HE_x and HE_y modes

$$L = 2\pi/\delta\beta = \lambda/nB \tag{12}$$

are often used to express the magnitude of the birefringence [26]. In (12), λ and n denote the free-space wavelength and the refractive index of the fiber material, respectively. When the beat length L is much shorter than the typical spatial period of geometrical perturbations in the fiber (bends, for example), the energy transfer between the HE_x and HE_y modes is effectively suppressed.

The third scheme, proposed first by Jeunhomme and Monerie [40], is a version of the birefringent fiber which should be called the "circularly birefringent" or "circularly single-polarization" fiber.

Fig. 12 compares the principles of the linearly SPSM and circularly SPSM fibers. A linearly SPSM fiber (Fig. 12(a)) has an axially-nonsymmetrical structure or internal stress to make the propagation constants of the two orthogonal HE_{11} modes, β_x and β_y, different from each other, thus decoupling these modes. In a circularly SPSM fiber (Fig. 12(b)), twist is given to an axially symmetrical fiber to decouple the clockwise and counter-clockwise circular polarizations, taking advantage of twist-induced optical activity. In this case the degree of decoupling is again given as the difference in the propagation constants, and is proportional to the twist angle per unit length φ (see Fig. 12(b)).

In the following subsections, the above three types are described in some detail.

C. Birefringent Fiber Having Axially-Nonsymmetrical Refractive Index Distribution

A typical example is an elliptical-core fiber. However, analysis showed that the birefringence obtained with an elliptical core fiber was not strong enough [31]. The first experiment was reported in 1978 by Ramaswamy *et al.* [32], who fabricated a fiber having a dumbbell-shaped core. The beat length L was typically 55 mm [30], [32], whereas it was believed that L should be less than 1 mm to make it well below the typical perturbation periods that can exist in actual fibers.

One method for reducing L is to increase the relative index difference Δ ($\Delta = (n_1^2 - n_2^2)/2n_1^2 \doteqdot (n_1 - n_2)/n_1$ where n_1 and n_2 are core and cladding indexes, respectively), because the theory predicts that $L \propto B^{-1} \propto \Delta^{-2}$.

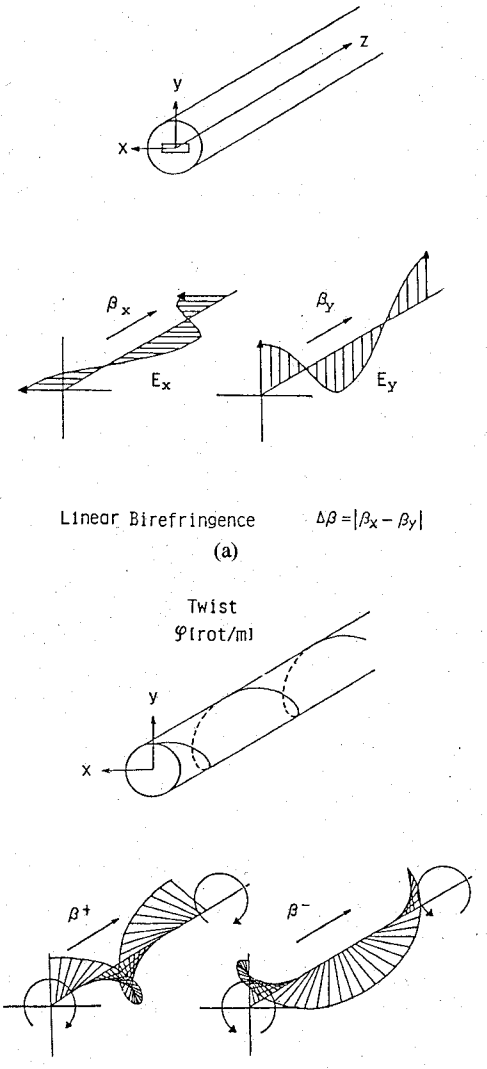

Fig. 12. Principles of the SPSM fibers. (a) Linearly SPSM fiber. (b) Circularly SPSM fiber.

Actually, it was shown later by Dyott *et al.* that L as short as 0.75 mm could be obtained by increasing Δ to 4.3 percent [33].

However, engineers believe that increasing Δ too much would not be practical because the transmission loss would increase and the connection and splicing would become difficult (note that the core radius must be reduced when Δ increases). Thus, an alternative way described in the following is being pursued.

D. Stress-Induced Linearly Birefringent Fibers

An elliptical-core fiber exhibits more or less an anisotropic birefringence caused by axially nonsymmetrical mechanical stress produced in the drawing process because the melting-point temperature and thermal expansion coefficient are different for core and cladding materials. At first this effect was not used intentionally. However, since 1978, various deformed-cladding schemes have been proposed for deliberately enhancing such stress-induced birefringence to obtain higher B and shorter L [34]–[39].

The method employed first to produce a deformed cladding was to machine the preform in an axially nonsymmetrical form before it is drawn to a fiber. The lowest value of L reported in 1979 was 1.3 cm for $\Delta = 0.0054$ and at $\lambda = 442$ nm [36]. In 1980, achievement of $L = 0.83$ mm was reported by Matsumura *et al.* [37], with a fiber having $\Delta = 0.0045$ and at $\lambda = 633$ μm. This fiber has a circular core, circular inner cladding, elliptical outer cladding, and circular jacket, and features the lowest loss ever reported (0.8 dB/km at $=1.55$ μm) for stress-induced birefringent fibers.

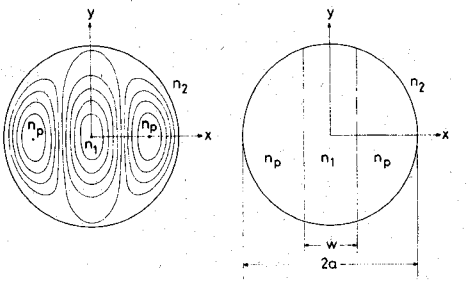

Fig. 13. Refractive-index distribution with two pits on either side of core. (a) Smooth distribution. (b) Step-index distribution (in both cases $n_p < n_2 < n_1$).

TABLE I
COMPARISION OF LINEARLY AND CIRCULARLY SPSM FIBERS (AS TO THE POLARIZATION DISPERSION, SEE [26])

	Lin. SPSM	Circ. SPSM
Fabrication	Difficult	Easy
Polarization stability	Probably better	Probably poorer
Connection	Difficult	Easy
Polarization dispersion	Large	Small
Polarization matching with LO injection	Necessary	Unnecessary

E. Circularly Birefringent Fibers

Table I shows the comparison of the features of linearly SPSM and circularly SPSM fibers. The latter shows many attractive features. However, the minimum obtained beat length is several centimeters for the circularly SPSM fiber; this is almost two orders of magnitude longer than that in the linearly SPSM fiber. We should continue, therefore, the research on both approaches at least for the time being.

F. Side-Pit Fiber and Side-Tunnel Fiber

A hint for realizing an absolutely SPSM fiber can be found in the following fact: in an axially *symmetrical* fiber having an "index valley" with appreciable width and depth around the core, a cutoff region appears for the HE_{11} mode [41]. We may then predict that, in the index distributions as shown in Fig. 13, where $n_1 > n_2 > n_p$, the HE_x and HE_y modes will have different cutoff frequencies, producing an absolutely SPSM region between them.

At first it was assumed that $\Delta_p = (n_2 - n_p)/n_2$ would never exceed several percent because of the material limitation. Such fibers with relatively shallow refractive-index

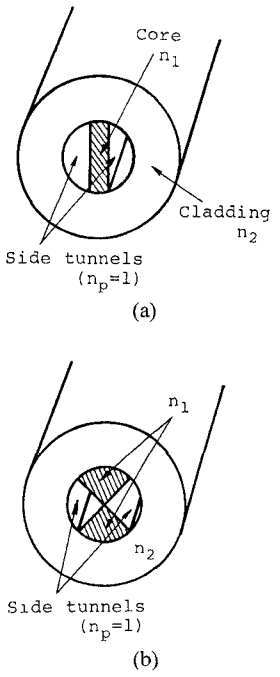

Fig. 14. Two examples of the side-tunnel fiber.

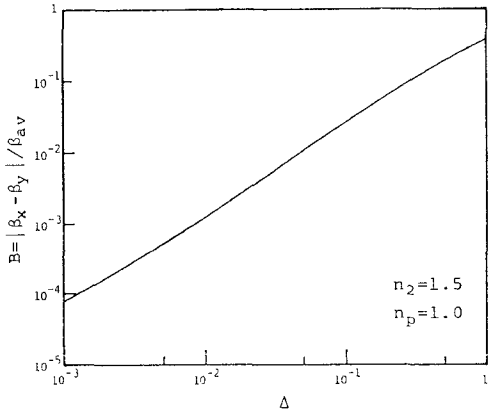

Fig. 15 The relative birefringence B of a side-tunnel structure of Fig. 14(a), as a function of the relative index difference Δ.

pits were named side-pit fibers [27], and samples were manufactured by Hosaka *et al.* [28]. However, it was also found that the relative single-polarization bandwidth $S(=(v_{cx}-v_{cy})/v_{c,\mathrm{av}}$, where v_{cx} and v_{cy} are the normalized cutoff frequencies and $v_{c,\mathrm{av}}=(v_{cx}+v_{cy})/2)$ is rather narrow; S is typically only 0.024 for the case $\Delta=\Delta_p=0.01$, and $S\propto\Delta$. Thus, the side-pit fiber actually fabricated [28] could be used merely as a strongly birefringent fiber rather than an absolutely single-polarization one.

To overcome this limitation, a new structure called a "side-tunnel fiber" has been proposed, which features two "side tunnels" (where $n_p=1$) as shown in Fig. 14(a) instead of the side index pits. In such a structure, the relative bandwidth could be widened appreciably, for example, $S=0.07$ for $\Delta=0.01$, and $S=0.17$ for $\Delta=0.05$ (It is assumed that $W=0.3\times(2a)$ and $n_p=1$ in Fig. 13(b).) Furthermore, by designing the cross-sectional shape of the core more properly, for example as shown in Fig. 14(b), the absolutely SMSM bandwidth can further be widened.

A side-tunnel fiber may of course be used as a strongly birefringent fiber. Fig. 15 shows the computed relative birefringence B at $v=v_{cx}$, for the structure shown in Fig. 14(a). This curve shows that $B=1.3\times10^{-3}$ and 2.7×10^{-2} for $\Delta=0.01$ and 0.1, respectively; these values of B are much higher than the maximum value reported so far: $B\doteqdot5\times10^{-4}$ [43]. The fabrication of side-tunnel fibers is in progress.

VII. System Experiment—Measurement of Bit-Error Rate

Finally, some results of the bit-error rate (BER) measurement of a heterodyne-type optical communication system will be presented.

Practically, the greatest problem in the BER measurement of a heterodyne system is that it takes a long time, sometimes as long as several hours. The presently available AFC technique is not yet so excellent as to assure an enough stability for such a long time.

Therefore, in the measurement reported so far, a "simulation" scheme [44] is employed. Fig. 16 shows the schematic diagram of a simulation model for the PCM–ASK heterodyne-type optical communication system. A part of the laser output is used as the local oscillator power. The other part, the signal power, is frequency-shifted by 40 MHz by using an acoustooptical modulator, and also amplitude-modulated with a pseudo-random pulse sequence (the M-sequence) of 150 kbit/s.

The optical attenuator stands for the fiber waveguide. The photodetector mixes the LO and signal frequencies. The output of the IF amplifier is filtered by a bandpass filter (bandwidth $W=1$ MHz), and demodulated by an envelope detector. The BER is measured as a function of the signal power P_s, with the local oscillator power P_{LO} as a parameter.

The maximum local oscillator power injected into the photodiode was 1.6 mW, which generated a photodiode current of 350 μA. The load resistance to the photodiode was 3 kΩ, and the noise figure F of the amplifier was approximately 3 dB. In such a case, the shot-noise current $(2eI_{\mathrm{LO}}W)$ predominates over the circuit-noise current $(=4kTFW/R)$ [5], where e is the electron charge, k the Boltzmann constant, T the circuit temperature, and W denotes the bandwidth.

Fig. 17 shows the result of the measurement [45]. Small circles, crosses, and dots show the measured BER for three different local oscillator power levels. When the quantum noise-limited operation is achieved, the BER of a ASK-heterodyne envelope detection system should be given as [5]

$$P_e=\frac{1}{2}\exp\left(-\frac{\eta P_s}{8eW}\right) \tag{13}$$

where η is the conversion factor from light power to photocurrent. The solid curve in Fig. 17 has been obtained by using (13) and using $\eta=0.21$ A/W. The theoretical and experimental BER curves show fairly good agreement when P_{LO} is sufficient; the difference ($\sim$1 dB) is probably due to the intensity noise of the local oscillator [45].

The BER measurement of a PCM–FSK system using

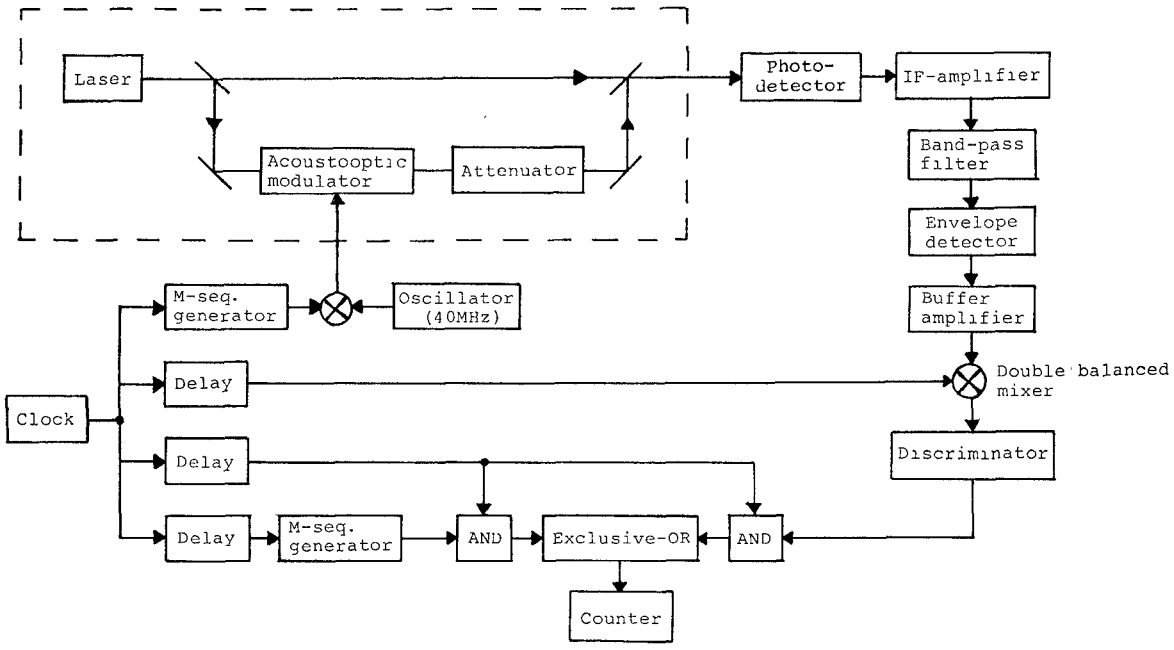

Fig. 16. A simulation model of a PCM–ASK heterodyne-type optical communication system for measuring the BER.

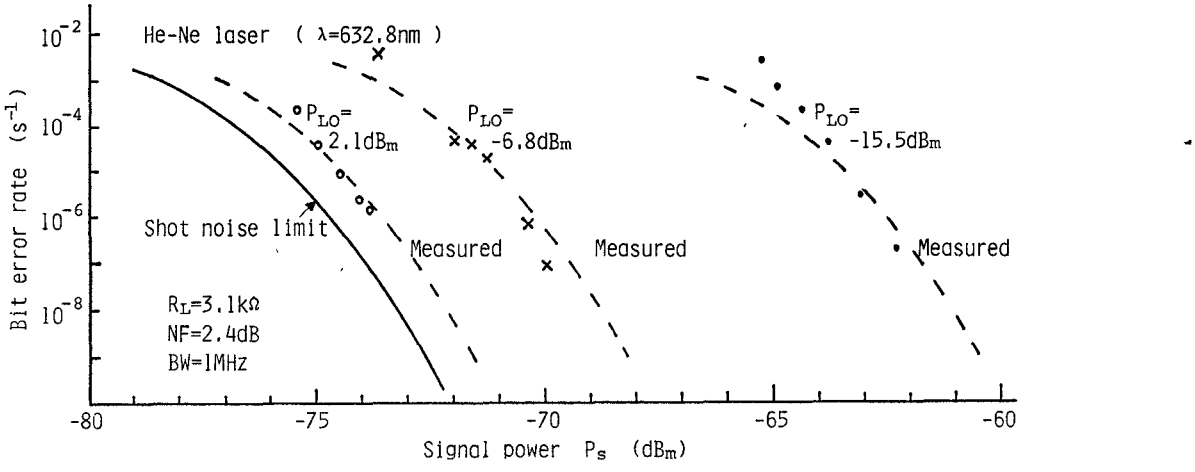

Fig. 17. Measured and theoretical bit-error rate of a PCM–ASK heterodyne-type optical communication system.

two independent, frequency stabilized lasers is in progress [46], but so far not reported. The measured BER is said to show a lower limit due to the oscillator noise. Preliminary heterodyne-detection experiment performed prior to the BER measurement is described in [47].

After the manuscript had been completed, the author was informed that the BER measurement has recently been performed also with a system using a GaAlAs laser preamplifier. The required signal level was found to be 10 dB above the quantum-noise limit (7 dB below Si APD direct detection) at wavelength of 0.85 μm [48]. In this experiment, however, the detector/amplifier system following the laser is not heterodyne type.

VIII. Conclusion

The technical significance, history of R and D, relevant tasks, and recent progress in heterodyne/coherent optical fiber communications have been reviewed. The result of the BER measurement indicates that, despite many technical difficulties, the heterodyne/coherent system is a promising and interesting technical target.

Appendix
Derivation of (1)

The output current of an ideal photodetector is given as $I_0 = eP_s/hf$ where e denotes the electron charge. When the load resistance is R_L, the above current produces signal power S and noise power N as

$$S = R_L(eP_s/hf)^2$$

$$N = R_L 2eI_0\Delta f = R_L(2e^2P_s/hf)\Delta f$$

which directly lead to (1) in the text.

References

[1] T. Okoshi, "Heterodyne-type optical fiber communications" in *Third IOOC Int. Conf. Integrated Opt. Optical Fiber Commun. Tech. Dig.*, (San Francisco, CA), Apr. 27–29, p. 44.

[2] T. Okoshi and K. Kikuchi, "Heterodyne-type optical fiber com-

munications," *J Opt. Comm.*, vol. 2, pp. 82–88, Sept. 1981.
[3] O. E. DeLange, "Wideband optical communication systems: Part II —Frequency division multiplexing," *Proc. IEEE*, vol. 58, pp. 1683–1690, (see page 1687), Oct. 1970.
[4] T. Okoshi, "Feasibility study of frequency-division multiplexing optical fiber communication systems using optical heterodyne or homodyne schemes," (in Japanese) *Pap. Tech. Group IECE Japan*, no. OQE 78-139, Feb. 27, 1979. (Japanese specialists had the first open discussion on this topic at this meeting.)
[5] T. Okoshi, K. Emura, K. Kikuchi, and R. Th Kersten, "Computation of bit-error rate of various heterodyne and coherent-type optical communication schemes," *J. Opt. Comm.*, vol. 2, no. 3, pp. 89–96, Sept. 1981.
[6] Y. Yamamoto, "Receiver performance evaluation of various digital optical modulation-demodulation syst. in the 0.5-10-μm-wavelength region," *IEEE J. Quantum Electron.*, vol. QE-16, pp. 1251–1259, Nov 1980.
[7] D. Marcuse, *Engineering Quantum Electronics*. New York: Harcourt Brace, 1970, ch 6.
[8] S. Stein and J. J. Jones, *Modern Communication Principles*. New York: McGraw Hill, 1965
[9] R. G. Smith and S. D. Personick, "Receiver design for optical fiber communication system," in *Semiconductor Devices for Optical Communication*, H. Kressel, Ed. Berlin: Springer, 1980, ch. 4.
[10] Y. Yamamoto and T. Kimura, "Coherent optical fiber transmission systems," *IEEE J. Quantum Electron.*, vol. QE-17, pp. 919–935, June 1981.
[11] F. Favre, L. Jeunhomme, I. Joindot, M. Monerie, and J. C. Simon, "Progress towards heterodyne-type single-mode fiber communication syst.," *IEEE J. Quantum Electron.*, vol. QE-17, pp. 897–906, June 1981.
[12] T. Okoshi and K. Kikuchi, "Frequency stabilization of semiconductor lasers for heterodyne-type optical communication schemes," *Electron Lett.*, vol. 16, pp. 179–181, Feb. 28, 1980.
[13] K. Kikuchi, T. Okoshi, and M. Kawanishi, "Achievement of 1 MHz frequency stability of semiconductor lasers with double-stage AFC scheme," *Electron Lett*, vol. 17, pp. 515–516, July 23, 1981.
[14] F. Favre and D. LeGuen, "High frequency stability of laser diode for heterodyne communication systems," *Electron. Lett.*, vol 16, pp. 709–710, Aug. 28, 1980.
[15] F Favre and D. LeGuen, "Laser diode emitter for heterodyne-type communication systems," in *Third IOOC Int. Conf. Integrated Opt. Optical Fiber Commun. Tech. Dig.* (San Francisco, CA), p 34.
[16] H. Tsuchida, M. Ohtsu, and T. Tako, "Frequency stabilization of AlGaAs semiconductor lasers to the absorption line of water vapor," *Pap. Tech Group IECE Japan*, no. OQE81-74, Sept. 28, 1981.
[17] H. Hori *et al.*, "Frequency stabilization of a diode laser on a saturated absorption spectrum," *Pap Tech. Group IECE Japan*, no. OQE81-73, Sept 28, 1981.
[18] T. Yabuzaki *et al*, "Frequency locking of a GaAlAs laser to a Doppler-free spectrum of the Cs-D_2 line," *Japan J. Appl. Phys.*, vol. 20, no. 6, pp L451–L454, June 1981.
[19] H. Tsuchida, M. Ohtsu, and T Tako, "Frequency stabilization of AlGaAs DH lasers," *Japan J. Appl. Phys.*, vol. 20, pp. L403–L406, June 1981.
[20] T. Okoshi, K Kikuchi, and A Nakayama, "Novel method for high resolution measurement of laser output spectrum," *Electron. Lett.*, vol. 16, pp. 630–631, July 31, 1980.
[21] S. Saito and Y. Yamamoto, "Direct observation of Lorentzian line-shape of semiconductor laser and linewidth reduction with external grating feedback," *Electron. Lett.*, vol. 17, pp. 325–327, Apr. 30, 1981.
[22] K. Kikuchi and T. Okoshi, "Simple formula giving spectrum narrowing ratio of semiconductor-laser output obtained by optical feedback," *Electron. Lett.*, vol. 18, pp. 10–11, Jan. 7, 1982.
[23] R. Ulrich, "Polarization stabilization on single-mode fiber," *Appl. Phys. Lett.*, vol. 35, no. 12, pp. 840–842, Dec. 1979.
[24] M Kubota, T. Ohhara, K Furuya, and Y. Suematsu, "Electrooptical polarization control on single-mode optical fibers, *Electron. Lett.*, vol. 16, no. 15, p 573, July 17, 1980.
[25] H. C. LeFevre, "Single-mode fiber fractional wave devices and polarization controllers," *Electron. Lett.*, vol. 16, no 20, pp 778–780, Sept. 25, 1980.
[26] T. Okoshi, "Single-polarization single-mode optical fibers," *IEEE J. Quantum Electron*, vol QE-17, pp 879–884, June 1981
[27] T. Okoshi and K. Oyamada, "Single-polarization single-mode optical fiber with refractive-index pits on both sides of core" *Electron. Lett.*, vol. 16, no. 18, pp. 712–713, Aug. 28, 1980.
[28] T. Hosaka, K. Okamoto, Y. Sasaki, and T. Edahiro, "Single-mode fibers with asymmetrical refractive-index pits on both sides of core," *Electron Lett.*, vol. 17, no. 5, pp. 191–193, Mar. 5, 1981.
[29] T. Okoshi and K. Oyamada, "Proposal and analysis of side-tunnel optical fibers," *Pap. Tech. Group IECE Japan*, no. OQE82-38, July 29, 1982.
[30] V. Ramaswamy, W. G. French, and R. D. Standley, "Polarization characteristics of noncircular core single-mode fiber," *Appl. Opt.*, vol 17, no. 18, pp. 3014–3017, Sept. 15, 1978.
[31] M. J. Adams, D. N. Payne, and C. M. Ragdale, "Birefringence in optical fibers with elliptical cross-section," *Electron. Lett.*, vol. 15, no. 10, pp. 298–299, May 10, 1979.
[32] V Ramaswamy and W. G. French, "Influence of noncircular core on the polarization performance of single-mode fibers," *Electron. Lett.*, vol. 14, no. 5, pp. 143–144, Mar. 2, 1978.
[33] R. B. Dyott, J. R. Cozens, and D. G. Morris, "Preservation of polarization in optical-fiber waveguides with elliptical cores," *Electron. Lett.*, vol. 15, no. 13, pp. 380–382, June 21, 1979.
[34] R. Ramaswamy, I. P. Kaminow, and P Kaiser, "Single polarization optical fibers: Exposed cladding technique," *Appl. Phys. Lett.*, vol. 33, no. 9, pp 814–816, Nov. 1, 1978.
[35] R. H. Stolen, V. Ramaswamy, P. Kaiser, and W. Pleibel, "Linear polarization in birefringent single-mode fibers," *Appl. Phys. Lett.*, vol. 33, no. 8, pp. 699–701, Oct. 15, 1978.
[36] V. Ramaswamy, R H. Stolen, M. D. Divino, and W. Pleibel, "Birefringence in elliptically clad borosilicate single-mode fibers," *Appl. Opt.*, vol. 18, no. 24, pp. 4080–4084, Dec. 15, 1979.
[37] H. Matsumura, T. Katsuyama, and T. Suganuma, "Fundamental study of single polarization fibers," in *Proc. 6th ECOC Euro. Conf. Opt Comm. Tech. Dig.*, (York, U.K.), pp. 49–52, Sept. 16–19, 1980. Also, private communication from H. Matsumura
[38] J. P Kaminow, J. R. Simpson, H. M. Presby, and J B. MacChesney, "Strain birefringence in single-polarization germanosilicate optical fibers," *Electron Lett.*, vol. 15, no. 21, pp. 677–679, Oct. 11, 1979.
[39] T. Hosaka, K. Okamoto, T. Miya, Y. Sasaki, and T. Edahiro, "Low-loss single-polarization fibers with asymmetrical strain birefringence," *Electron. Lett.*, vol. 17, no. 15, pp. 530–531, July 23, 1981
[40] L. Jeunhomme and M. Monerie, "Polarization-maintaining single-mode fiber cable design," *Electron. Lett.*, vol. 16, no 24, pp 921–922, Nov. 20, 1981.
[41] K. Okamoto and T. Okoshi, "Analysis of wave propagation in optical fibers having core with α-power refractive-index distribution and uniform cladding," *IEEE Trans. Microwave Theory Tech.*, vol. MTT-24, pp 416–421, July 1976.
[42] K. Oyamada and T. Okoshi, "Two-dimensional finite-element method calculation of propagation characteristics of axially nonsymmetrical optical fibers," *Radio Sci.*, vol. 17, no. 1, pp. 109–116, Jan.–Feb. 1982.
[43] Data shown in [33] and [37]. The data obtained so far are summarized and compared in a review paper [26].
[44] K. Kikuchi, T Okoshi, and J. Kitano, "Measurement of bit-error rate of heterodyne-type optical communication system—A simulation experiment," *IEEE J. Quantum Electron*, vol. QE-17, pp. 2266–2267, Dec. 1981.
[45] K. Kikuchi, T. Okoshi, and K. Emura, "Achievement of nearly shot-noise-limited operation in a heterodyne-type PCM-ASK optical communication system," *8th ECOC, Euro. Conf. Opt. Comm.*, (Canne, France), Sept. 21–24, 1982.
[46] Y. Yamamoto, private communication.
[47] S. Saito, Y. Yamamoto, and T. Kimura, "Optical FSK heterodyne detection experiments using semiconductor laser transmitter and local oscillator," *IEEE J. Quantum Electron.*, vol. QE-17, pp 935–941, June 1981.
[48] Y. Yamamoto, private communication. Also see T. Mukai, Y Yamamoto, and T. Kimura, "S/N and error-rate performance in AlGaAs semiconductor laser preamplifier and linear repeater systems," submitted to *IEEE J Quantum Electron*

Takanori Okoshi (S'56–M'60) was born in Tokyo, Japan, on September 16, 1932. He received the B.S., M.S., and Ph.D. degrees, all from the University of Tokyo, Tokyo, Japan, in 1955, 1957, and 1960, respectively, all in electrical engineering.

In 1960 he was appointed an Instructor, and in 1961, became an Associate Professor in the Department of Electronic Engineering, University of Tokyo, where he worked primarily in the field of microwave circuits, microwave measurements, and microwave electron devices. From 1963 through 1964, on leave of absence from the University of Tokyo, he joined Bell Laboratories, Inc., Murray Hill, NJ, where he was engaged in research on electron guns. In 1972 he joined the Technical University of Munich on a temporary basis as a Guest Professor. In January 1977 he became a Professor at the University of Tokyo. At present, his main fields of interest are optical fibers, optical fiber communications, three-dimensional imaging, microwave planar (two-dimensional) circuits, and holographic memories. He has written nine books, including two in English entitled *Three-Dimensional Imaging Techniques* (New York. Academic PreSs, 1976), and *Optical Fibers* (Academic Press, 1982). He has been awarded nine prizes from three Japanese academic institutions.

Dr. Okoshi is a Guest Research Fellow of Radio Research Laboratory of Japanese Government and the Secretary of Japanese National Committee for URSI.

Clinical RF Hyperthermia by Magnetic-Loop Induction: A New Approach to Human Cancer Therapy

F. KRISTIAN STORM, ROBERT S. ELLIOTT, FELLOW, IEEE, WILLIAM H. HARRISON, MEMBER, IEEE, AND DONALD L. MORTON

Invited Paper

Abstract—**There has been mounting laboratory evidence that temperatures of $\geq 42°C$ (108°F) are tumoricidal in tumor cell cultures and animal models. Localized heat by electromagnetic waves appears to be the most practical means for producing hyperthermia and has been shown to be potentially effective against human surface tumors. However, attempts to treat deep internal human cancers with available techniques have been either ineffective or dangerous because of injury to surface tissue.**

A fundamentally new approach, magnetrode magnetic-loop induction hyperthermia, which was cooperatively developed by electrical engineers and oncologists for the treatment of deep-seated human tumors, is the subject of this report. The concept, rationale, design, and performance of this applicator in phantoms, animals, and humans is presented, as are the early results of clinical cancer trials. The data suggest reason for enthusiasm for the future treatment of advanced human tumors.

Manuscript received March 12, 1982. This paper was supported in part by the National Cancer Institute, DHEW under Grant CA 24883, and in part by the Medical Research Service of the Veterans Administration.

F. K. Storm and D. Morton are with the Division of Oncology, Department of Surgery, UCLA School of Medicine, University of California, Los Angeles, CA 90024, and Surgical Service, Veterans Administration Hospital, Sepulveda, CA 91343.

R. S. Elliott and W. M. Harrison are with the Department of Electrical Sciences and Engineering, UCLA School of Engineering and Applied Sciences, University of California, Los Angeles, CA 90024.

I. INTRODUCTION

ONE IN four Americans has or will develop cancer, but only one in three will be cured of their disease by present methods of therapy, including surgery, radiation therapy, chemotherapy, and immunotherapy. Thus, oncologists must seek additional safe and reliable methods of treatment, particularly for large internal solid tumors. Initial investigations from laboratory models, animals, and human clinical trials suggest that hyperthermia may have a significant place in the armamentarium against this disease.

At $\geq 42°C$ (108°F), there is irreversible damage to cancer cell respiration [1], [2]. Coincident alterations occur in

0018-9480/82/0800-1149$00.75 ©1982 IEEE